

Magnetic fluid under vorticity: Free precession decay of magnetization and optical anisotropy

F. Gazeau,¹ B. M. Heegaard,¹ J.-C. Bacri,^{1,*} A. Cebers,² and R. Perzynski¹

¹*Laboratoire d'Acoustique et Optique de la Matière Condensée, Université Pierre et Marie Curie, Tour 13, Boite 78, 4 place Jussieu, 75252 Paris Cedex 05, France*

²*Latvian Academy of Sciences, Institute of Physics, LV-2169, Salaspils-1, Latvia*

(Received 14 March 1996)

We submit a magnetic fluid to a solid rotation and analyze the free precession decay of its transverse magnetization and of its nondiagonal optical anisotropy. In agreement with the theoretical predictions, they present damped oscillations because the magnetic particles rotate, dragged by the carrier angular velocity. The node period is inversely proportional to vorticity. We show that magnetic particles can be used as advanced nanoscopic tools to probe neatly the vorticity of their fluid carrier. [S1063-651X(96)04310-3]

PACS number(s): 47.32.-y, 75.50.Mm, 42.25.Lc

Under time-dependent magnetic fields, spectacular effects are observed with concentrated magnetic fluids (MF's) such as unexpected drop instabilities (starfishes) [1] or surprising hydrodynamic properties (negative rotational viscosity) [2,3]. They are due to the asymmetry of the MF stress tensor. Dilute magnetic fluids also deserve a growing interest. In several pioneer experiments, magnetic particles have been used as nanoscopic probes [4–8] of their surrounding medium. The basic idea is that the measurable macroscopic properties of the magnetic medium—as magnetization or optical anisotropy—give a direct picture of the local particle response, coupled to the carrier, to an external magnetic field [9–11]. As soon as the chemical compatibility between the magnetic particles and the tested medium is ensured, a study of the hydrodynamic or of the rheology of the fluid carrier is possible [11]. As they are suspended in tiny concentrations, nanoscopic grains do not perturb the fluid structure or its motion on larger scales. Furthermore, the magnetic and magneto-optic responses of the particles are contactlessly driven by an external parameter: the magnetic field. They are detected through noninvasive methods: standard magnetization measurements perform an average over the whole sample; optical measurements are more local, the average being performed only over the cross section of the laser beam. Besides, the main strength of this new probing is the spatial range of the measurement. The particles get an insight into the carrier matrix on their own spatial scale, of the order of a few nanometers. It gives us a great opportunity to investigate intrinsic structures and kinetics of complex fluids that are not scale invariant. For example, viscoelastic measurements have been performed during sol-gel transitions using this method [5,7]. For a better understanding of scale effects in turbulent flows [12], it turns out that probes at nanoscales should bring real improvements. The magnetic particles are directly sensitive to the local fluid vorticity, unlike other methods involving the measurement of two adjunct velocities to deduce the velocity gradient [13–15]. Thus, even though the measurement volume is determined by the experi-

mental device, the spatial scale corresponding to the hydrodynamic volume of the particles, is resolved.

In this paper, we focus on the magnetic and magneto-optic responses of a magnetic fluid in a vortical flow. If immersed in a steady magnetic field H , the magnetic moments $\vec{\mu}_p$, carried by the MF particles, tend to align along the field, leading to a macroscopic magnetization M of the suspension. Moreover, a mechanical reorientation of the particles themselves is induced, if the magnetic moments are rigidly bound to the particle bodies. Each particle being optically anisotropic, its optical axis \vec{n} is also parallel to the magnetic moment $\vec{\mu}_p$. If no return force drags the particles, the equilibrium magnetization lies along the field. This is the case if particles are suspended in a quiescent liquid. In a flowing liquid, on the contrary, the magnetic field pins the orientation of particles within the fluid. A viscous-drag torque arises conversely owing to the difference between the angular velocity of the particles and the local angular velocity of the surrounding liquid $\Omega = (\nabla \times \vec{v})/2$. To compensate this torque induced by the flow, the magnetic torque $M \times H$ has some finite value. It entails a component of the magnetization normal to the applied field. The link between vorticity and magnetization is explicitly shown here, by measuring the transient magnetic response of the MF, after the field is switched off. Inside the flowing liquid and after the magnetic field is removed, the particles undergo a solid rotation with the fluid angular velocity Ω . On short times, coherent rotation of the magnetic moments arises together with the particle mechanical rotation. Therefore, the magnetization vector precesses about the vorticity axis, with the angular velocity Ω . However, in competition, the Brownian rotational motion has a disordering effect on the particles. After a characteristic time τ , the orientation of the particles, and hence of their magnetic moments, is randomized, leading to a net zero magnetization. It should be noted that orientational fluctuations, rather than positional ones, are relevant. A “rotational” Peclet number can be introduced, defined as $Pe_R = \Omega\tau$. It is the ratio of the magnetization relaxation time to the characteristic time of fluid deformations.

In a quiescent fluid, the relaxation of the magnetization has been described by the postulated equation [9,10]

$$\frac{d\vec{M}}{dt} = -\frac{\vec{M} - \vec{M}_0}{\tau}, \quad (1)$$

*Also at Université Paris 7, UFR de Physique, 2 Place Jussieu 75251 Paris Cédex 05, France.

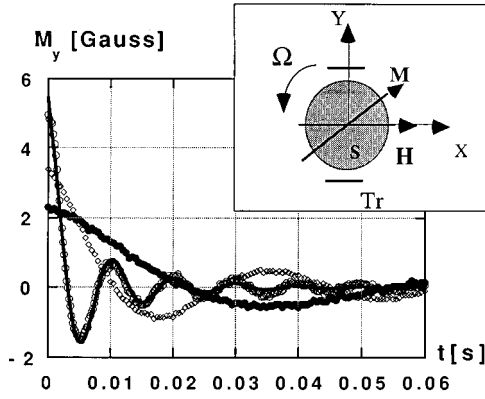


FIG. 1. Experimental relaxation of magnetization M_y as a function of time for different values of vorticity Ω (\circ , $\Omega=628$ rad/s; \diamond , $\Omega=182$ rad/s; \bullet , $\Omega=93$ rad/s). The solid line corresponds to the fit for $\Omega=628$ rad/s using a stretched exponential (see text): $\tau_0=3.3\times 10^{-3}$ s and $\beta=0.63$. Inset: Experimental setup for the detection of the transverse magnetization (Tr, Hall transducers; S, MF sample rotating at angular velocity Ω).

where \vec{M}_0 is the equilibrium magnetization. Here, in zero field, $\vec{M}_0=\vec{0}$.

In a fluid with a local vorticity $\vec{\Omega}$ and in the framework of linear response, this last equation is transformed into

$$\frac{d\vec{M}}{dt} = -\frac{\vec{M}-\vec{M}_0}{\tau} + \vec{\Omega} \times \vec{M} \quad (2)$$

structurally analogous to Bloch equations. The second term holds for the solid rotation of the particle bodies and hence of the macroscopic magnetization.

In the present paper we test experimentally the validity of this equation by measuring the free precession decay (FPD) of magnetization. Moreover, we demonstrate that a local vorticity measurement is possible via the analysis of the FPD of the MF optical anisotropy.

Free precession decay of magnetization under a rotational flow

The magnetic fluid used here is an ionic ferrofluid synthesized through the Massart method. The grain magnetic material is cobalt ferrite with magnetization $M_S=3.6\times 10^5$ A/m. The large anisotropy constant ($K=2\times 10^5$ J/m³) of this ferrite ensures that the magnetic moment carried by a particle is ‘‘locked’’ to the crystalline structure in the easy direction. Thus, the magnetic moment rotates together with the particle body and the optical anisotropy axis [16]. The carrier liquid is glycerol with viscosity $\eta=1$ Pa s. For particles of magnetic diameter 10 nm, it yields experimental relaxation times of the order of 10 ms. The volume fraction of magnetic particles is $\Phi=1.5\%$.

The experimental setup of the magnetic detection is illustrated by the inset of Fig. 1. The vorticity of the fluid $\Omega=(0,0,\Omega)$ originates from the solid rotation of a cylindrical tube (length, 3 cm; diameter, 0.8 cm), containing the MF. A pulsed magnetic field $H=(H(t),0,0)$ with $H=1.6\times 10^4$ A/m is applied. The field pulses are long enough so that the magnetization of the suspension can reach its equilibrium value. The information is detected after removing the field, during the magnetization relaxation. We use Hall effect transducers

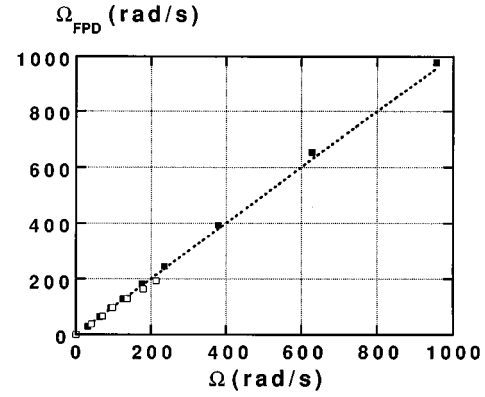


FIG. 2. Vorticity deduced from the free precession decay of magnetization (\blacksquare) and optical anisotropy (\square) as a function of the angular velocity of the motor. The dashed straight line features the relation $\Omega_{\text{FPD}}=\Omega$.

to measure the projection M_y of the magnetization vector along the y direction, normal to the field and to the vorticity.

Assuming that at $t=0$, the fluid has reached its equilibrium magnetization, $M_y(t>0)$ can be deduced from Eq. (2):

$$M_y(t) = \frac{\chi H}{\sqrt{1+\Omega^2\tau^2}} \exp(-t/\tau) \sin(\Omega t + \varphi) \quad (3)$$

with χ the initial susceptibility of the MF and $\tan \varphi=\Omega\tau$. The angle φ gives the magnetization equilibrium orientation with respect to an applied constant field H , in the presence of a vorticity Ω of the carrier fluid.

In Fig. 1, the free precession decay of the transverse magnetization M_y is shown for different values of the cylinder angular velocity Ω ($\Omega=628, 182, 93$ rad/s). While relaxing towards zero, M_y presents oscillations in agreement with expression (3). The period between two consecutive nodes must be compared to the half period of the fluid rotation $T/2=\pi/\Omega$. In Fig. 2, the vorticities Ω_{FPD} deduced from the nodes of the FPD signal are compared with the measured angular velocity Ω of the tube containing the MF. They coincide with good accuracy. Figures 1 and 2 show that the fluid vorticity is directly and easily measurable if two nodes can be observed. It supposes that the fluid vorticity should be faster than the relaxation of the magnetization under thermal fluctuations. In other words, the fluid must keep in memory its magnetized state longer than a period of fluid rotation. According to expression (3), there is no theoretical restriction to observe several nodes with the frequency of the fluid vorticity. The only limitation lies in the sensitivity of the measurement. In our experimental situation, we will retain the condition $Pe_R=\Omega\tau>1$, which is the criterion to obtain a maximum in the Fourier transform of the FPD signal. Figure 3 is an illustration of the signal $|M_y(\omega)|$ detected with the same experimental device, using a weak alternating magnetic field $(H_0\cos\omega t,0,0)$. $|M_y(\omega)|$ presents a sharp maximum for $\omega=\Omega$, in qualitative agreement with expression (2). The comparison of whole experimental curves in Figs. 1 and 3 to Eqs. (3) and (2) requires a precise knowledge of the magnetization relaxation processes. However, independently of τ , the FPD method provides a direct vorticity measurement by determination of the relaxation nodes. With this magnetic

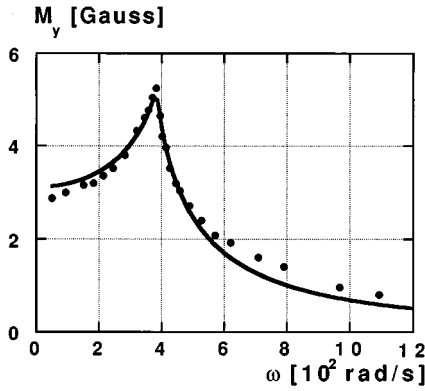


FIG. 3. Transverse magnetization M_y under solid rotation ($\Omega = 384$ rad/s) and alternating magnetic field ($H_0 = 6 \times 10^3$ A/m). Modulus $|M_y|$ as a function of the field frequency ω . The solid line corresponds to the fit using the Cole-Cole expression (see text): $\tau'_0 = 7.6 \times 10^{-3}$ s and $\alpha = 0.7$.

detection, the extension of the volume probed is limited by the dimension of the Hall or magneto-resistive probes (minimum 1 mm^3) and by their sensitivity. The optical FPD method that we will describe now, gets rid of these limitations. It is a local measurement, which is appropriate for a noninvasive investigation of highly dilute transparent suspensions.

Free precession decay of optical anisotropy: Towards a local measurement of vorticity

Under a flow, the magnetization acquires a component transverse to the applied field. In the same way, the optical anisotropy tensor of an elementary fluid volume acquires nondiagonal components. A vorticity measurement was recently developed according to this mechanism [8]. The nondiagonal term of the equilibrium anisotropy tensor, under a constant and large applied magnetic field, was measured locally through an optical method. However, this measurement, to be accurate, requires an independent determination of the relaxation time of the optical anisotropy. Here, we use a similar experimental setup, as presented in the inset of Fig. 4, with a pulsed field $H = (H(t), 0, 0)$ of weak amplitude ($H = 6.4 \times 10^3$ A/m). The polarized laser beam is parallel to the vorticity vector. Prior to crossing the rotating sample and to be analyzed, the laser beam is phase modulated at 50 kHz by a photoelastic modulator. The device provides a signal proportional to the nondiagonal component of the anisotropy tensor, according to Ref. [8]: $I/I_0 = S_{xy}$. We classically define the anisotropy tensor S_{ik} by $S_{ik} = 3/2(\langle n_i n_k \rangle - 1/3 \delta_{ik})$ where $\langle n_i n_k \rangle$ describes the mean angular orientation of the optical anisotropy. In the limit of weak fields, S_{ik} simplifies to $S_{ik} = \frac{3}{2} b H^2(t) (h_i h_k - \frac{1}{3} \delta_{ik})$ with $b = \frac{1}{15} (\mu_0 \mu_p / kT)^2$ (μ_0 vacuum permeability). As for the magnetization in Eq. (1), the evolution of S_{ik} in a quiescent fluid is approximated, for weak fields, by a simple exponential relaxation of characteristic time τ_a : $\dot{S}_{ik} = -(1/\tau_a)(S_{ik} - S_{ik}^{(0)})$. In the FPD experiment, $S_{ik}^{(0)}$ represents the equilibrium tensor towards which S_{ik} is relaxing: $S_{ik}^{(0)} \equiv 0$. In a fluid with a local vorticity Ω , an expression strictly analogous to Eq. (2) for magnetization, can be written for the anisotropy tensor:

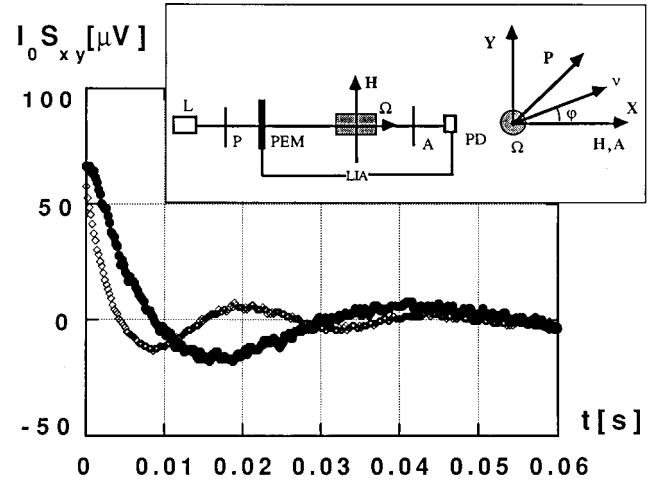


FIG. 4. Experimental relaxation of the nondiagonal component of the anisotropy tensor ($I_0 S_{xy}$): (\diamond $\Omega = 143$ rad/s; \bullet , $\Omega = 71$ rad/s). Inset: Experimental setup for optical detection with the respective directions of polarizer P , analyzer A , photoelastic modulator PEM (X, Y), magnetic field H , vorticity Ω of the rotating sample, and optical axis \vec{v} . LIA, lock-in amplifier; PD, photo-diode.

$$\frac{dS_{ik}}{dt} = -\frac{1}{\tau_a} (S_{ik} - S_{ik}^{(0)}) + (e_{ilm} \Omega_l S_{mk} + e_{klm} \Omega_l S_{im}) \quad (4)$$

with e_{ikl} the unit antisymmetric tensor. Assuming the same initial terms as for magnetization, namely, a saturated anisotropy at $t=0$ for the evolution of the nondiagonal component S_{xy} under a rotational flow and in zero field, we obtain the following equation:

$$S_{xy}(t) = \frac{bH^2}{4\sqrt{1 + (2\Omega\tau_a)^2}} \exp(-t/\tau_a) \sin(2\Omega t + \varphi'), \quad (5)$$

where $\tan \varphi' = 2\Omega\tau_a$. As expected, this equation corresponds directly to Eq. (3). The factor of 2 before the vorticity Ω and the even dependence on field H arise since we are dealing with the orientation of the optical axis, which obviously has no direction. From Eq. (5), we are able to estimate a value for the vorticity directly from the period between nodes for any relaxation time τ_a . In Fig. 4, the measured FPD of S_{xy} is plotted for two angular velocities Ω , 71 and 143 rad s^{-1} . In both cases, the vorticity can be directly estimated from the period $T_0/2$ between two consecutive nodes, we find, respectively, $\Omega = \pi/T_0 = 71$ and 142 rad s^{-1} . In the same way as for the magnetization measurements, a correlation between such optical determinations of Ω and the known angular velocity of the motor is presented in Fig. 2.

To sum up, we have checked experimentally, in a MF under vortical flow, the general predictions of expressions (2) and (4), for the FPD of the magnetization and of the optical anisotropy. The FPD is directly sensitive to the fluid local vorticity through the solid rotation of the suspended nanoscopic magnetic particles. In contrast to the former experiment of Ref. [8], using magnetic particles under a constant magnetic field, the present vorticity measurement can be fully decoupled from the study of detailed relaxation processes and of the microscopic particle characteristics.

This is of great importance since we may point out the complexity of these relaxation processes. For example, in the recordings of Figs. 1 and 4, the relaxation is not a pure exponential. A correct adjustment of the FPD experimental curves requires, for example, a stretched exponential $\exp[-(t/\tau_0)^\beta]$ in both expressions (3) and (5). A typical example is given in Fig. 1 for $\Omega=628$ rad/s. For clarity, only one fit is presented: though β is approximately a constant ($\beta \approx 0.65$), the associated relaxation time τ_0 is a decreasing function of Ω . In the same way, in the frequency domain, the response $|M_y(\omega)|$ to an alternating field is satisfactorily adjusted if a Cole-Cole form is assumed for the susceptibility: $\chi(\omega) = \chi/[1 + (i\omega\tau_0')^\alpha]$ with $\alpha=0.7$ (cf. Fig. 3). These observations, which evidence a large distribution of relaxation times, could mirror the structural state of the MF.

Recent numerical works [17,18] on dipolar fluids predict the possible existence of some dynamical internal structures—chains of dipoles aligning nose to tail such as ‘living polymers’—if the isotropic attractive energy of the colloid is below a specific threshold. Preliminary results of small-angle neutron scattering (performed in Laboratoire Léon Brillouin, CEN Saclay, France) show that in the MF used here, the electrostatic repulsion between particles, which balances the attractive interactions, is strong enough to preserve the colloidal stability but less efficient than for other aqueous ferrofluids made of $\gamma\text{-Fe}_2\text{O}_3$ particles [19]. It lends some support to the existence of local particle correlations in the present MF. They could generate long relaxation times, field dependent, and could contribute to the time distribution that is observed. These effects will be discussed in detail in forthcoming papers. Nevertheless, our vorticity measurement does not depend on this distribution and the

only limitation for an accurate vorticity determination is that the rotational Peclet number must be larger than one. It means that high vorticity flows optimize this determination.

Regarding the optical detection, the present technique holds out against all the other noninvasive methods of vorticity or gradient velocity measurements [13–15,20,21]. The spatial resolution is limited only by the cross section of the laser beam probing the fluid. The spatial scale of the measurement is determined by the hydrodynamic volume V_h of particles, or small chains of particles, if any, which remain in the global range $10^3\text{--}10^5$ nm³. The time resolution is given by the orientational diffusion time of the rotating optical axis. This time (from 10^{-6} to 10^{-1} s depending on V_h and for a viscosity of the carrier fluid in the range $10^{-3}\text{--}1$ Pa s) is much smaller than the translational diffusion time of photochromic tracers involved in the forced Rayleigh scattering method [20,21], for instance. The promising future of the optical vorticity measurement presented here, is an easy two-dimensional (2D) mapping of vortical flows. A 3D investigation should be possible if a pin-pointed magnetic field, perpendicular to the vortex, is locally induced.

We are greatly indebted to Dr. S. Neveu for providing us with the MF sample and to J. Servais for his technical assistance. We are grateful to Y. Couder and V. Croquette who first pointed out the interest of MF in local vorticity measurements, and to M. Shliomis for fruitful discussions. This work was supported by ‘Le Réseau Formation–Recherche’ No. 90R0933 of MENESRIP and by the International Science Foundation (Grant No. L7Q100). The Laboratoire d’Acoustique et Optique de la Matière Condensée is associated with the Centre National de la Recherche Scientifique.

-
- [1] J. C. Bacri, A. Cebers, and R. Perzynski, *Phys. Rev. Lett.* **72**, 2705 (1994).
- [2] R. E. Rosensweig, *Science* **271**, 614 (1996).
- [3] J. C. Bacri, R. Perzynski, M. I. Shliomis, and G. I. Burde, *Phys. Rev. Lett.* **75**, 2128 (1995).
- [4] H. W. Davies and J. P. Llewellyn, *J. Phys. D* **12**, 311 (1979).
- [5] J.-C. Bacri and D. Gorse, *J. Phys. (Paris)* **44**, 985 (1983).
- [6] J.-C. Bacri, J. Dumas, D. Gorse, R. Perzynski, and D. Salin, *J. Phys. Lett. (France)* **46**, L-1199 (1985).
- [7] J.-C. Bacri, B. M. Heegaard, R. Perzynski, and D. Zins, *Braz. J. Phys.* **25**, 127 (1995).
- [8] B. M. Heegaard, J.-C. Bacri, R. Perzynski, and M. Shliomis, *Europhys. Lett.* **34**, 299 (1996).
- [9] R. E. Rosensweig, *Ferrohydrodynamics* (Cambridge University Press, Cambridge, 1985).
- [10] M. I. Shliomis, T. P. Lyubimov, and D. V. Lyubimov, *Chem. Eng. Comm.* **67**, 275 (1988).
- [11] E. I. Blums, A. O. Cebers, M. M. Maiorov, and B. Nicoaru, *Magn. Gidrodin.* **1**, 53 (1987) (in Russian).
- [12] Z. S. She, E. Jackson, and S. A. Orszag, *Nature* **344**, 226 (1990).
- [13] J. C. Agui and J. Jimenez, *J. Fluid Mech.* **185**, 447 (1987).
- [14] G. G. Fuller, J. M. Rallison, R. L. Schmidt, and L. G. Leal, *J. Fluid Mech.* **100**, 555 (1980).
- [15] J. J. Wang, D. Yavich, and L. G. Leal, *Phys. Fluids* **6**, 3519 (1994).
- [16] S. Neveu, F. Tourhino, J.-C. Bacri, and R. Perzynski, *Colloids Surf. A* **80**, 1 (1993).
- [17] M. E. van Leeuwen and B. Smit, *Phys. Rev. Lett.* **71**, 3991 (1993).
- [18] M. J. Stevens, and G. S. Grest *Phys. Rev. Lett.* **72**, 3686 (1994).
- [19] J.-C. Bacri, F. Boué, V. Cabuil, R. Perzynski, *Colloids Surf. A* **80**, 11 (1993).
- [20] M. Cloitre, E. Guyon, *J. Fluid Mech.* **164**, 217 (1986).
- [21] J. G. A. Garcia and L. Hesselink, *Phys. Fluid A* **2**, 688 (1990).